Available online at www.sciencedirect.com
ScienceDirect
Bioelectrochemistry 73 (2008) 155–162
Bioelectrochemistry
www.elsevier.com/locate/bioelechem

Structural and functional changes in the membrane and membrane skeleton of red blood cells induced by peroxynitrite

Maria N. Starodubtseva [a,*], Amanda L. Tattersall [b], Tatyana G. Kuznetsova [a], Nicolai I. Yegorenkov [c], J. Clive Ellory [b]

[a] Gomel State Medical University, Lange str., 5, 246000 Gomel, Belarus
[b] Department of Physiology, Anatomy and Genetics, University of Oxford, Sherrington Building, Parks Road, Oxford OX1 3PT, United Kingdom
[c] Gomel State Technical University, Oktyabrya ave., 48, 246746 Gomel, Belarus

Received 15 May 2007; received in revised form 16 December 2007; accepted 17 January 2008
Available online 5 February 2008

Abstract

The changes in passive ion permeability of the red blood cell membrane after peroxynitrite action (3 μM–3 mM) have been studied by biophysical (using radioisotopes of rubidium, sodium and sulphur (sulphate)) and electrophysiological methods. The enhancement of passive membrane permeability to cations (potassium and sodium ions) and the inhibition of anion flux through the anion exchanger in peroxynitrite-treated red blood cells were revealed. In patch-clamp experiments the whole-cell conductance after peroxynitrite (80 μM) treatment of red blood cells increased 3–3.5-fold with a shift in the reversal potential from −7.0±1.5 mV to −4.3±0.9 mV ($n=7$, $p=0.005$). The addition of cobalt and nickel ions to red blood cell suspensions before peroxynitrite treatment had no effect on the peroxynitrite-induced cation flux but zinc ions in the same condition decreased cation flux about 2-fold. Using atomic force microscopy methods we revealed an increase in red blood cell membrane stiffness and the membrane skeleton complexity after peroxynitrite action. We conclude that the peroxynitrite-induced water and ion imbalance and reorganization in membrane structure lead to crenation of red blood cells.

Keywords: Peroxynitrite; Red blood cell; Passive cation and anion transport; Membrane reorganization; Atomic force microscopy

1. Introduction

Peroxynitrite is formed during many pathological processes in the human organism such as ischemia, inflammation, neurodegenerative diseases, and diabetes [1–5]. Peroxynitrite, alongside other reactive oxygen species (ROS), affects the ion permeability of the cell membrane, which appears to be an important element of the mechanisms of cellular functions [6,7]. Peroxynitrite not only oxidizes lipids, nucleic acids, protein SH-groups but also nitrites aromatic amino acid residues of proteins [5,8]. The properties of peroxynitrite provide many opportunities for regulating cellular ion transport system activity—both directly through protein structure modification and indirectly with participation of various regulatory factors [8–11].

Peroxynitrite is either peroxynitrous acid (HOONO) or the peroxynitrite anion ($ONOO^-$, $pK_a=6.8$ at 37 °C). Peroxynitrite can be synthesized in reactions with the participation of pairs—either $NO/{}^{\cdot}O_2^-$ or HNO_2/H_2O_2 [5,12]. The $ONOO^-$ anion is relatively stable, while HOONO decays rapidly. At physiological pH, the apparent half-life of peroxynitrite is about 1 s. Formation of a reactive intermediate with CO_2 ($ONOOCO_2^-$) leads to a decrease in the half-life of peroxynitrite (0.5–3 ms) [5]. Red blood cells (RBCs) are considered as a major 'sink' of ${}^{\cdot}NO/NO_2^-$ in human blood [13,14]. Recently it was discovered that the RBCs could express a functional endothelial nitric oxide synthase [15], so that under certain conditions RBCs can produce peroxynitrite itself. Moreover RBCs can be exposed to exogenous peroxynitrite generated by other cells. Many events that occurred in RBCs or with RBC components under peroxynitrite action have already been studied.

* Corresponding author. Department of Biological and Medical Physics, Gomel State Medical University, Lange str., 5, 246000 Gomel, Belarus. Tel.: +375 232 745274; fax: +375 232 749831.
E-mail address: starodubtseva_mn@hotmail.com (M.N. Starodubtseva).

1567-5394/$ - see front matter © 2008 Elsevier B.V. All rights reserved.
doi:10.1016/j.bioelechem.2008.01.008

They include haemoglobin oxidation, inactivation of RBC enzymes, changes in active and passive ion transports, in membrane skeleton component state and so on [7,16–24]. Herein, we investigate the changes in passive ionic permeability of RBC membrane after peroxynitrite action and the structural changes in RBC membrane and membrane skeleton.

2. Materials and methods

2.1. Peroxynitrite synthesis

Peroxynitrite was synthesized using the methods described by Beckman et al. with some modifications [12]. Briefly, an ice-cold, flowing solution of 1.2 M $NaNO_2$ was entrained with an equal volume of 1.2 M H_2O_2 acidified by 0.6 M HNO_3, and the resultant mixture then dripped into a solution of NaOH (at a final concentration of 0.5 M). The solution was filtered through granular MnO_2 and frozen at −20 °C for up to a week. The final concentration of peroxynitrite was determined by absorbance at 302 nm in 1 M NaOH ($\varepsilon_{302\ nm}$=1670 M^{-1} cm^{-1}) with a spectrophotometer. An inactive control solution containing decomposed peroxynitrite was produced when NaOH was added to the mixture of $NaNO_2$ and H_2O_2 after a 30 min delay period.

2.2. Blood samples

Blood samples were obtained by venepuncture of healthy donors, with permission under ethical consent, and collected into heparinized syringes. Samples were kept at 4 °C until use within 72 h. The blood was washed three times by centrifugation (2000 g; 10 min) in appropriate buffered saline solution. Plasma and buffy coat were removed by aspiration. Haematocrit was measured by the cyanomethemoglobin method. The ATP level in RBCs was measured by using Micro Beta chemiluminometer and ATP light kit (Perkin Elmer). The ATP concentration of normal RBCs was 1.3±0.1 mM (n=6).

2.3. Ion influx measurements

For flux experiments peroxynitrite was added to the RBC suspension in buffered saline 10 min before both radioisotope-containing solution injection and the addition of the inhibitors of transport systems.

K^+ influx in RBCs was determined at 37 °C using $^{86}Rb^+$ as a congener, added in KNO_3 to give a final K^+ concentration of 7.5 mM [25]. Before K^+ influx measurement cells were incubated with a buffer solution containing 10 mM glucose and 10 mM inosine for 1 h at 37 °C and washed 3 times with buffer solution without sucrose and inosine. For $^{86}Rb^+$ flux experiments phosphate buffered saline was used (PBS) (in mM): NaCl (100), Na_2HPO_4/NaH_2PO_4 (50), pH 7.4 at 37 °C. In chloride-free experiments nitrate PBS was used in which the chloride was replaced by nitrate ($NaNO_3$). 100 μM Ouabain, 10 μM bumetanide and 10 μM clotrimazole (Sigma Chemical Corp.) were present in the solutions during all flux experiments. 4,4′-Diisothiocyanato-2,2′-stilbene-disulphonic acid (DIDS) (100 μM), $ZnCl_2$ (100 μM), $NiCl_2$ (100 μM), $CoCl_2$ (100 μM) (Sigma Chemical Corp.) were added to the RBC suspension before peroxynitrite injection and $^{86}Rb^+$ addition. *p*-Chloromercuribenzene sulfonate (pCMBS) (1 mM), tetraethylammonium chloride (TEA) (3,5 mM), tolbutamide (200 μM), 6-chloro-9-[(4-diethylamino)-1-methyl-buthyl]amino-2-methoxyacridine dihydrochloride (quinacrine) (100 μM) (Sigma Chemical Corp.) were added to the RBC suspension after peroxynitrite but before $^{86}Rb^+$ addition. K^+ influxes are expressed in standard units of mmoles K^+/l cells·h or relative units as a ratio of K^+ influx under the test conditions compared to K^+ influx of peroxynitrite-treated cells.

Na^+ influx in RBC was determined at 37 °C. $^{22}Na^+$ was diluted in $NaNO_3$ to give a final Na^+ concentration of 150 mM and a radioactivity of 0.1 μCi/ml cell suspension. Protocol followed that for K^+ influx measurement.

Anion influx into RBCs through anion exchanger (AE1) was estimated at 30 °C using $^{35}SO_4^{2-}$ to give a final sulphate concentration of 4 mM in a RBC suspension of 20% Hct. For $^{35}SO_4^{2-}$ flux experiments citrate buffer saline was used (in mM): $Na_3C_6H_5O_7$ (84), EGTA (1), pH 6.5 at 37 °C. After 5 min incubation of 100 μl of RBC suspension with $^{35}SO_4^{2-}$ 10 μl of 40 μM DIDS solution was added to stop the anion influx.

2.4. Electrophysiology

Membrane currents were recorded using whole-cell configurations. Patch pipettes (tip resistances 10–13 MΩ) were prepared from borosilicate glass capillaries pulled and polished on a Werner Zeitz DMZ programmable puller (Augsburg, Germany). The bath solution contained (mM): MOPS (or HEPES) (10), NaCl (145), $CaCl_2$ (5) at pH 7.4. The pipette solution was a high-potassium solution. The ruptured patch whole-cell voltage-clamp configuration was used to record membrane currents. RBC membrane seals (>2 GΩ) were obtained by the application of suction to the pipette (1–2 kPa) followed by the imposition of a negative pipette potential (−5 to −30 mV). Cell rupture was attained by a short burst of strong suction and the configuration was assessed by a decrease in access resistance and the development of a small capacitance transient. Whole-cell currents were recorded using an Axopatch 200A amplifier, with voltage command protocols generated and the currents were analyzed using the pCLAMP software suite (Version 8, Axon Instruments Inc., USA). Whole-cell *I–V* curves were obtained by evoking a series of test potentials from −100 to +100 mV in 10 mV steps for 300 or 500 ms from a holding potential of 0 or −10 mV. Membrane slope-conductance (g) at positive and negative potentials were estimated by calculating the averaged gradient of *I–V* curves in the ranges of 30–80 mV (for g_+) and (−30)-(−80) mV (for g_-), and also at −10 mV (which approximates to erythrocyte resting membrane potential). For patch-clamp experiments peroxynitrite was added as a bolus (an aliquot of concentrate solution) to the bath after reaching the seal and recording currents of normal RBC state. Haematocrit of red blood cell suspension was approximately 0.001%. All experiments were performed at room temperature. In all cases, n denotes the number of cells tested.

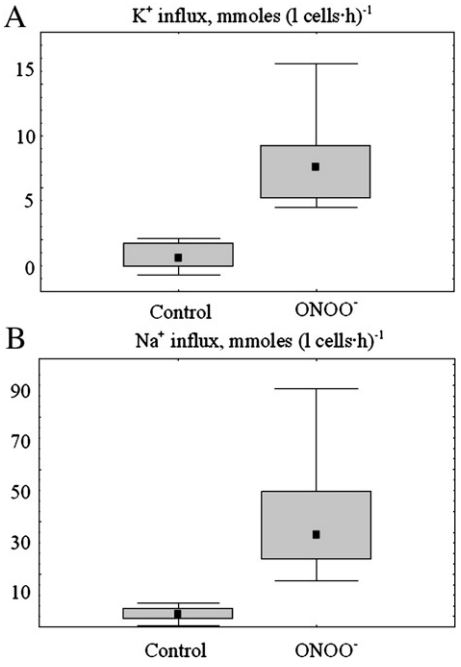

Fig. 1. The effect of peroxynitrite on K^+(A) and Na^+(B) influx in red blood cells. $Na^+$and K^+ influxes in RBC were measured at 37 °C for 10 min using correspondingly $^{22}Na^+$ and $^{86}Rb^+$ as a congener of K^+. Peroxynitrite concentration was 1 mM, K^+ concentration was 7.5 mM. The haematocrit of RBC suspension was 5%, pH 7.4. The symbols, boxes and whisker represent median values, 25%−75% percentile boundaries, minimal and maximal values. $n=9$.

2.5. Atomic force microscopy of RBC surface and analysis of atomic force microscopy results

For atomic force microscopy (AFM) investigations peroxynitrite was added to whole blood (pH = 7.4 ± 0.2, Hct = 41 ± 3%, $n=8$) as a bolus (an aliquot of concentrate solution). RBCs were fixed with 1% glutaraldehyde in PBS at room temperature, washed firstly by phosphate buffer 3 times, then by distilled water 3 times. RBCs were placed on a glass base plate for further study of their surface by using the contact AFM mode. AFM scanning was performed with atomic force microscope "NT-206" (MicroTestMachines Co., Belarus) using standard AFM tips (CSC38 and NSC11) (MikroMasch). Topography and torsion images were recorded. After analyzing the field of the size of 8×8 μm^2 a small part of RBC surface of 1×1 μm^2 was analyzed. The scanning step did not exceed 2 nm that permitted the observation of fine features of the RBC surface. Observation was carried out in air at room temperature. Changes in torsion angle (lateral force maps) provide evidence of the alteration in composition or mechanical properties of the surface and subsurface layers. The lateral force map of fixed RBC surface perfectly reflects the underlining membrane skeleton structure. We used some image filters to contrast the membrane skeleton structure image. The fractal dimension of the lateral force map (D_F) of size of 1×1 μm^2 was used for quantitative evaluation of the complexity of the skeleton structure. The fractal dimension was calculated with the area-perimeter method based on the correlation law between perimeter (L) and area (A) for islands (or lakes) on the analyzed surface [26]: $L \propto A^{(D_F-1)/2}$.

Two hundred "levels" between the minimal and maximal vertical heights in the image were used. The fractal dimension was calculated from the least-square linear regression line in a log–log plot of the perimeter versus area with the program "SurfaceXplore 1.3.11" (MicroTestMachines Co., Belarus). Apparent elastic modulus of RBC surface layers was estimated from the dependence of AFM cantilever deflection on the tip indentation depth using Hertz's model.

2.6. Statistics

The fit of data distribution to a normal distribution was checked by Shapiro–Wilk's W test. The normally distributed data are represented as the limits of confidence interval (CI) and the number (n) of the experiments. The data that were not in accord with normal distribution are represented in the figures as a median, 25% and 75% percentile boundaries, maximal and minimal values, and the number (n) of the experiments. The comparisons between the samples were carried out by using either two-tailed Student t test or Wilcoxon matched test.

3. Results

3.1. Peroxynitrite increases passive cation permeability of the RBC membrane

Peroxynitrite treatment of RBCs leads to an increase in both potassium ion influx and sodium ion influx (Fig. 1). The effect of peroxynitrite on cation flux through the RBC membrane depends on the level of haematocrit present in the RBC suspension. The peroxynitrite-induced K^+ and Na^+-influxes both increase with decreasing haematocrit in the RBC suspension. At the same time the ATP level decreases after peroxynitrite treatment of the RBCs (Fig. 2), but this is not the explanation for the peroxynitrite effects since ATP repletion with glucose/inosine did not alter the response to peroxynitrite (data not shown).

3.2. The interaction of anion exchanger with peroxynitrite

There are two known ways for peroxynitrite to penetrate the RBC membrane. They are (i) transport of peroxynitrite anion

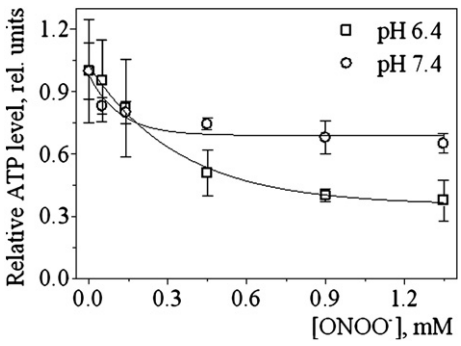

Fig. 2. The effect of peroxynitrite on relative ATP levels in red blood cells. The ATP level in RBCs was measured by using Micro Beta chemiluminometer and ATP light kit (Perkin Elmer). The haematocrit of RBC suspension was 5%. The findings are represented as the limits of confidence interval ($n=4$–8).

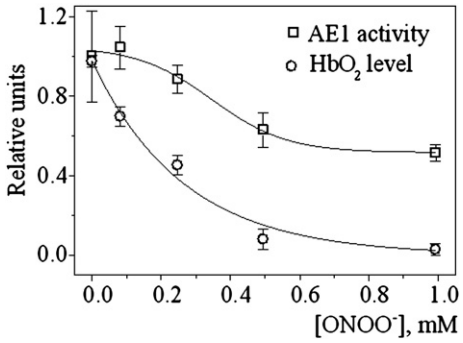

Fig. 3. The effect of peroxynitrite on anion exchanger (AE1) activity and oxyhemoglobin (HbO_2) level in red blood cells. Anion influx into RBCs through AE1 was estimated at 30 °C using $^{35}SO_4^{2-}$ in citrate buffer, pH 6.5. The haematocrit of RBC suspension was 20%. Haemoglobin concentration was measured in haemolysates by spectrophotometry (OD_{541}, OD_{630}). The findings are represented as the limits of confidence interval (n=4–8).

through AE1 and, (ii) simple diffusion of peroxynitrous acid through the lipid bilayer. Denicola and colleagues showed there was a 50% decrease in intracellular methaemoglobin level when RBCs were treated with 300 μM peroxynitrite and an inhibitor of AE1 (DIDS, 100 μM) (Hct<0.5%, pH 6.8) [22]. The influence of DIDS on the ability of peroxynitrite to induce K^+-influx in RBCs was thus examined. DIDS was found to inhibit peroxynitrite-induced K^+-influx in RBCs (Hct 5%) in a dose-dependent manner. 100 μM DIDS decreased peroxynitrite-induced K^+-influx (1 mM) by 2.5-fold. In addition, our findings also demonstrate that peroxynitrite can inhibit the activity of AE1 dose-dependently (Fig. 3). Peroxynitrite (1 mM) decreases anion flux in RBCs (Hct 20%, pH 6.5) about 2-fold. Unfortunately, the inhibition of AE1 by peroxynitrite is observed at concentrations higher than needed for complete haemoglobin oxidation (Fig. 3). Haemoglobin is known to be an important enhancer of peroxynitrite action on RBCs due to its reaction with peroxynitrite in which a number of other ROS are produced [24].

3.3. The interaction between transition metal ions and peroxynitrite-induced cation influx in RBCs

The transition metal ions catalyze the oxidation reactions with the participation of ROS either themselves or in complexes like haem [27–29]. Iron, copper, cobalt, and nickel ions initiate the cascade of lipid peroxidation in the Fenton reaction with the participation of OH-radicals. OH-radical is one from the products of peroxynitrite transformation in cells [5]. The action of Co^{2+} and Ni^{2+} ions on the ability of peroxynitrite to enhance the cation flux into RBCs was therefore looked at. Co^{2+} and Ni^{2+} ions were introduced into the reactive solutions 5 min before peroxynitrite addition. Neither Co^{2+} nor Ni^{2+} ions have an influence on the level of peroxynitrite-induced K^+ influx into RBCs (Fig. 4, A). The ability of zinc ions to influence the oxidative processes induced by peroxynitrite in RBCs was also examined. Zn^{2+} ions are considered to be an antioxidant in different oxidative processes [27]. Zinc can protect the protein sulphydryls against oxidation and reduce the formation of OH-radicals from H_2O_2 through the antagonism of redox-active transition metals [30]. The effect of Zn^{2+} ions on the ability of peroxynitrite to enhance the cation flux into RBCs strongly depends on individual donors. In general, Zn^{2+} ions can protect RBCs against peroxynitrite-induced cation flux (Fig. 4, B). Zn^{2+} ion is also a known inhibitor of RBC cation channels and could also be acting by inhibiting cation uptake directly [31].

3.4. The effect of peroxynitrite on whole-cell current in RBCs

Whole-cell currents were recorded in response to voltage steps with MOPS-buffered saline in the bath and high-K^+ solution in the recording pipette. The seal resistance was 3.2±1.9 GΩ (CI, n=8) and the series resistance was 10.8±0.8 MΩ (CI, n=8). Under the control conditions RBCs displayed an outward current with the membrane current reversing polarity at the potential E_r=−7.0±1.5 mV (CI, n=7). Membrane slope-conductance (g) at positive and negative potentials was g_+=1573±532 pS and g_-=1170±476 pS (CI, n=8) respectively. Membrane conductance at −10 mV was 401±316 pS (CI, n=8). Membrane slope-conductance at positive potential and membrane conductance at −10 mV were in general agreement with the normal RBC membrane conductance values estimated

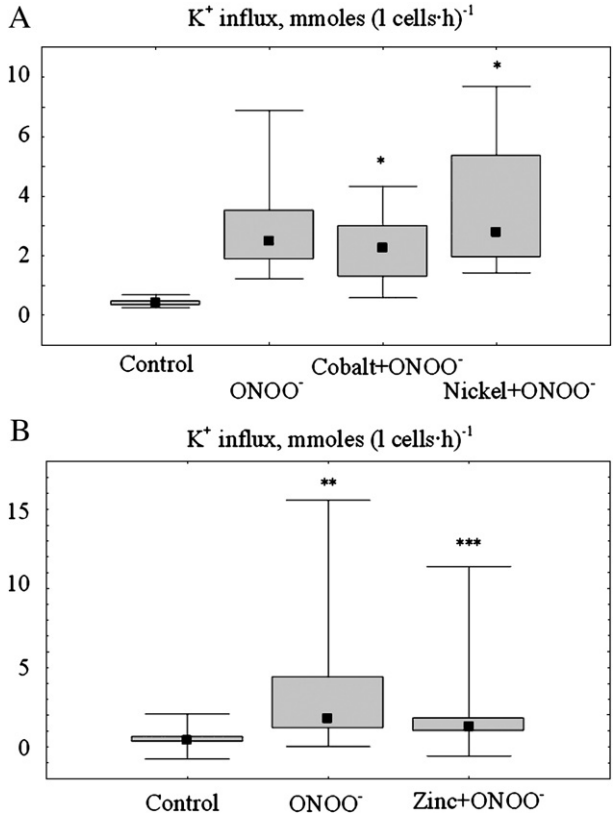

Fig. 4. The effect of cobalt, nickel (A) and zinc ions (B) on 1 mM peroxynitrite-induced K^+ influx in red blood cells. A: The haematocrit of RBC suspension was 2.1±0.8%, pH 7.4. n=18 (3 donors). *p>0.1 vs. $ONOO^-$ sample (Wilcoxon test) (N. S.). B: The haematocrit of RBC suspension was 3.7±0.8%, pH 7.4. n=53 (11 donors). **p<0.001 vs. control, ***p=0.001 vs. $ONOO^-$ sample (Wilcoxon test). The symbols, boxes and whisker represent median values, 25%–75% percentile boundaries, minimal and maximal values.

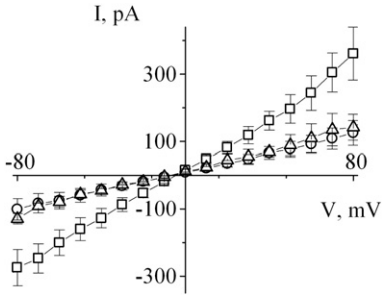

Fig. 5. The effect of peroxynitrite on whole-cell current in red blood cells. Current–voltage (*I–V*) relationships are plotted for currents sequentially recorded immediately after pipette break-in (circles, $n=8$), 10 min after addition of 80 μM peroxynitrite (squares, CI, $n=8$) or 10 min after addition of 80 μM decomposed peroxynitrite (triangles, CI, $n=3$). Bath solution was MOPS-buffered solution, pH 7.4, and pipette contained high-K^+ solution.

by Browning with coworkers, but membrane slope-conductance negative potential in our experiments was a little higher than the conductance estimated by them [31].

The RBCs treated by peroxynitrite before a patch-clamp experiment did not make good seals. The maximal seal resistance achieved was only 700–800 MΩ. To test the effect of peroxynitrite on whole-cell current the following protocol was used. Whole-cell seals were made on control cells then an 80 μM peroxynitrite was added to the bath. The current was recorded immediately after peroxynitrite injection and at an additional time interval, usually 10 min.

Peroxynitrite changes both inward and outward ionic currents through the RBC membrane (Fig. 5). Membrane conductance after 10 min peroxynitrite treatment increases 3–3.5-fold ($g_+=4147\pm508$ pS, $g_-=3262\pm376$ pS and $g(-10\text{ mV})=1817\pm497$ pS (CI, $n=8$)). The difference between currents of normal RBCs and of RBCs treated with decomposed peroxynitrite was not statistically significant (*t* test, $p>0.05$). The whole-cell I–V relation for peroxynitrite-treated erythrocytes showed a reversal potential at -4.3 ± 0.9 mV (CI, $n=7$, $p=0.005$ vs. control).

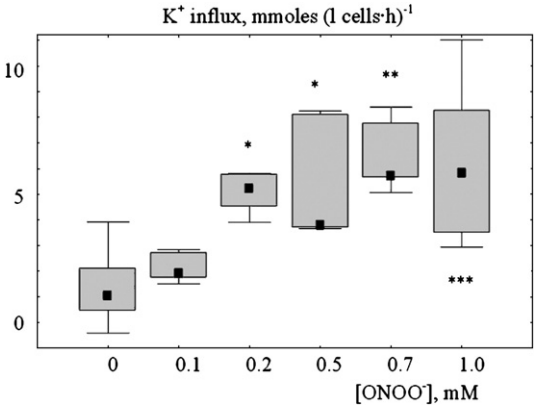

Fig. 6. The effect of peroxynitrite on Cl^--independent K^+ influx in red blood cells. The haematocrit of red blood cell suspension was 4.3±0.6%, pH 7.4. The symbols, boxes and whisker represent median values, 25%–75% percentile boundaries, minimal and maximal values. $n=6–36$. *$p<0.05$ vs. control, ** $p<0.01$ vs. control, ***$p<0.0001$ vs. control (Wilcoxon test).

Table 1
The effect of inhibitors of several transport systems on peroxynitrite-induced K^+ flux into red blood cell

Model	Types of inhibited transport systems	Ratio between K^+ flux and peroxynitrite-induced K^+ flux, rel. units
Peroxynitrite	–	1.00±0.10
Peroxynitrite+100 μM quinacrine	K^+/H^+ exchanger, nonspecific	1.24±0.06*
Peroxynitrite+200 μM tolbutamide	K_{ATP} channel	0.80±0.07*
Peroxynitrite+1 mM pCMBS	Water channel, nonspecific	6.82±0.05*
Peroxynitrite+3.5 mM TEA	Cation channel, nonspecific	2.88±0.12*

The data are represented as the limits of confidence interval (CI, $n=4–10$). *$p<0.001$ vs. $ONOO^-$ sample (two-tailed Student *t* test). The concentration of peroxynitrite is 1.07±0.09 mM. The haematocrit of RBC suspension was 5%, PBS, pH 7.4, 37 °C.

In the majority of cases, under the experimental conditions applied, the peroxynitrite treatment leads to consecutive loss of a seal (or haemolysis). This phenomenon can be caused by the disorder of the membrane structure under the peroxynitrite action that leads to the change of mechanical properties of the RBC membrane as a whole [23]. Before each loss of seal an enhanced ionic current was observed. The typical kinetic curve of ionic current at certain voltage steps was an exponential function (data not shown). Lower peroxynitrite concentrations also produce the disturbance in ionic current to a smaller extent and the effect is additive. Substituting K^+ ions in the recording

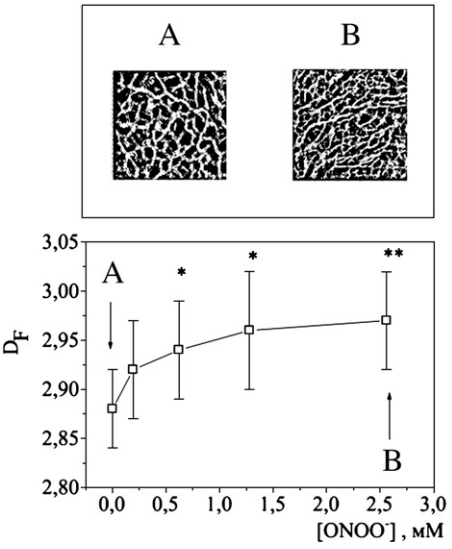

Fig. 7. The effect of peroxynitrite on red blood cell membrane skeleton structure. Bottom panel shows the fractal dimension of the lateral force maps of peroxynitrite-treated RBCs. Top panel represents the typical contrasted lateral force maps of control RBCs (a) and peroxynitrite-treated RBCs (b). The size of RBC areas is 1×1 μm^2. The arrows on the bottom panel show the peroxynitrite concentration ranges for the corresponding images of top panel. The findings are represented as the limits of confidence interval ($n=11–16$). *$p<0.05$ and **$p<0.01$ vs. control (two-tailed Student *t* test).

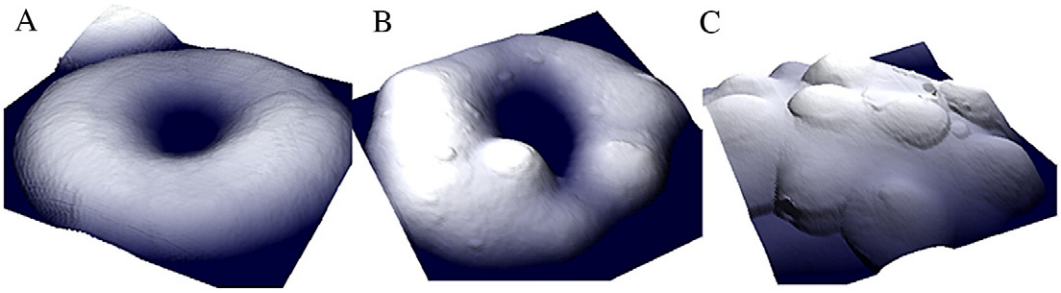

Fig. 8. Topography of red blood cells: discocytes (a), peroxynitrite-crenated cells of I type (b) and II type (c). RBCs were treated with peroxynitrite in whole blood (pH 7.4±0.2), fixed with glutaraldehyde, washed and dried. The tip CSC38 was used for AFM scanning of the RBC surface in contact mode.

pipette for non-permeable $NMDG^+$ ions decreases the peroxynitrite-induced ionic current.

3.5. The Cl^--independent K^+ flux induced by peroxynitrite action on RBCs

Peroxynitrite-induced K^+ influx into RBCs can be conventionally divided into Cl^--dependent and Cl^--independent K^+ influx [7]. We revealed that Cl^--dependent K^+ influx (determined by the activity of K^+–Cl^- cotransporter) developed at low peroxynitrite concentrations while Cl^--independent K^+ influx became apparent at peroxynitrite concentrations higher than about 200 μM. Cl-independent K^+ influx in RBCs increases with increasing peroxynitrite concentration (Fig. 6).

The nature of the Cl^--independent peroxynitrite-induced K^+ influx is still unclear. The effect of several inhibitors of K^+ transport systems on the peroxynitrite-induced K^+ influx into RBCs was examined. In our experiments, K^+ influx was measured in the presence of three inhibitors: ouabain (an inhibitor of Na^+/K^+ ATPase), bumetanide (an inhibitor of $NaKCl_2$ cotransporter) and clotrimazole (an inhibitor of Ca^{2+}-activated K^+ channels). In addition, pCMBS (a non-specific inhibitor of water channels), TEA (a non-specific inhibitor of cation and water channels), quinacrine (a non-specific regulator of cation transporters) and tolbutamide (an inhibitor of K_{ATP} channels) were used [32–34]. The findings are summarized in Table 1. TEA, pCMBS and quinacrine further enhance the cation influx in RBCs while tolbutamide partially (approximately by 20%) inhibits it.

3.6. The effect of peroxynitrite on RBC membrane skeleton structure

AFM study of the membrane and submembrane layers of single RBCs after treatment with peroxynitrite was performed. Analyzing together the topography and the lateral force maps of untreated and peroxynitrite-treated RBCs we observed changes in RBC submembrane structure. We revealed that the lateral force maps of fixed RBCs mirror the structure of membrane skeleton and additional application of image filters enhances the contrast of the images. The typical contrasted lateral force maps of the surfaces of untreated (control) and peroxynitrite-treated RBCs are represented in Fig. 7 (top panel). In most areas there was an increase of membrane skeleton structure density but in some regions there was a decrease. The fractal analysis of the lateral force maps showed that the complexity of membrane skeleton structure increases with increasing in peroxynitrite concentration (Fig. 7, bottom panel).

In AFM experiments we added peroxynitrite directly to whole blood. In whole blood, there are a lot of other targets, beside the RBCs, for peroxynitrite action such as plasma proteins [35], so the effective level of peroxynitrite to the RBCs actually was lower than stated.

3.7. The RBC membrane stiffness and RBC shape after peroxynitrite action

At peroxynitrite concentrations higher than about 300 μM in blood crenated forms of RBCs are observed. The number of

Table 2
The elastic properties of red blood cell membranes before and after peroxynitrite treatment

Experiment	Specimen	Indentation depth, nm	Relative elastic modulus (E/E_0), rel. units	p vs. control (two-tailed Student t test)	Sample size
1	Control discocytes	40	1.00±0.09	–	23
	Discocytes after peroxynitrite treatment	40	1.16±0.10	0.04	19
2	Control discocytes	14	1.00±0.09	–	8
	Crenated cells after peroxynitrite treatment (protrusion top)	14	1.20±0.07	0.02	8
	Crenated cells after peroxynitrite treatment (protrusion bottom)	14	1.27±0.21	0.002	5

E_0 is an apparent elastic modulus of the cellular surface of control RBCs; E is an apparent elastic modulus of the cellular surface of peroxynitrite-treated RBCs. The data are represented as the limits of confidence interval (CI).
RBCs were treated with 2.5 mM peroxynitrite in whole blood (pH 7.4±0.2, 41±3% Hct), fixed with glutaraldehyde, washed and dried.

crenated RBCs increases with peroxynitrite concentration and reaches about 22% at a peroxynitrite concentration of 2 mM. Firstly one or some isolated protrusions appear on the RBC surface (I type, Fig. 8, b), and then the number of the protrusions increases and reaches about 20 per cell (II type, Fig. 8, c). The averaged protrusion sizes are 1480±120 nm in diameter and 440±40 nm in height (n=34).

We estimated and compared the apparent local elastic moduli of RBCs before and after peroxynitrite treatment. As we had expected the stiffness of peroxynitrite-treated RBCs in both cases (without and with RBC shape changes) was significantly higher than that of control RBCs (Table 2).

The membrane skeleton is known to contribute to elastic properties of RBCs. Therefore the condensation of membrane skeleton structure has to increase the stiffness of RBC surface layers and to promote the RBC shape changes [36].

4. Discussion

Our work has demonstrated a variety of components of functional and structural responses of RBCs to peroxynitrite action. Peroxynitrite increases the passive cation permeability of the RBC membrane for both K^+ ions and Na^+ ions. The total membrane conductance after peroxynitrite treatment increased 2–3-fold. At the same time, peroxynitrite decreases anion flux through AE1. Bearing in mind that AE1 is one of the pathways transporting peroxynitrite into RBCs, it is important to note the following: the effect of AE1 inhibition by peroxynitrite occurs at high peroxynitrite concentrations and it does not have a significant influence on the oxidative processes in RBCs, such as haemoglobin oxidation. We should also note that RBC sample could be with a negligible contamination of leucocytes and platelets and it must be taken into account.

The mechanism for peroxynitrite-induced enhancement of RBC membrane cation permeability appears to be complex and involve multiple pathways. The regulation of transport systems by peroxynitrite can be through modification of protein and lipid chemical structures and through the rearrangement of protein and lipid structures in the membrane or membrane skeleton [6,23,37–39].

Thus, the peroxynitrite-induced increase in K^+ permeability can be due to at least two pathways. One pathway that appears at low peroxynitrite concentration relates to the activation of the K^+-Cl^- cotransporter via kinase inhibition [7,20,40]. Another pathway is observed at high concentrations of peroxynitrite and is probably related to both the activity of K^+ channels and to the formation of membrane structure defects. The type of K^+ channels that are activated by peroxynitrite provokes the curiosity of investigators. Probably they can be neither Ca^{2+}-dependent K^+channels nor potential-dependent K^+channels [7]. The possible candidates can be K_{ATP} channels taking into account the significant decrease in ATP level and sensitivity to K_{ATP} channel inhibitors [29]. Other possible candidates can be two-pore-domain K^+ channels [41]. According to our estimates based on results of experiments with K_{ATP} channel inhibitor the K^+ channels contribute to the increase of total passive membrane permeability after peroxynitrite treatment only about 20%. Therefore we concluded that rearrangements in the membrane and membrane skeleton of RBCs are mainly responsible for the phenomenon. Changes in membrane skeleton structure are an important consequence of peroxynitrite treatment and they also correlate with Cl^--independent K^+ influx, inhibition of AE1 activity, and decrease in ATP level. Peroxynitrite-induced changes in membrane skeleton structure lead to an increase in membrane stiffness that is detected even in discocytes before RBC shape change. The crenation of RBC seems to be a final link in the chain of events induced by peroxynitrite in RBCs. That is observed at high concentrations of peroxynitrite and appears to be caused by both water and ion imbalance between cell and surrounding medium and cytoskeletal structure changes. All these changes in the mechanical and structural properties of RBCs can lead to a rapid elimination of the cells from the circulation.

We conclude that peroxynitrite causes an enhancement of passive cation (potassium and sodium) permeability and inhibits the anion flux through anion exchanger in the RBC membrane. The mechanism of peroxynitrite-induced cation permeability is complex including activation of cotransporters and cation channels as well as membrane rearrangements. Zinc ions can protect RBC membrane against peroxynitrite-induced cation leak. Peroxynitrite changes the membrane skeleton structure in RBCs that is the basis of the increase of RBC surface stiffness. Peroxynitrite-induced processes in membrane and membrane skeleton lead to crenation of RBCs.

Acknowledgements

This work was partially supported by The Physiological Society.

The authors thank Kuznetsova T. A. and Abetkovskaya S. O. for technical help in carrying out several AFM experiments and calculation of elastic modulus.

References

[1] S. Cuzzocrea, D.P. Riley, A.P. Caputi, D. Salvemini, Antioxidant therapy: a new pharmacological approach in shock, inflammation, and ischemia/reperfusion injury, Pharmacol. Rev. 53 (1) (2001) 135–159.
[2] A. Denicola, R. Radi, Peroxynitrite and drug-dependent toxicity, Toxicology 208 (2) (2005) 273–288.
[3] D.M. McCafferty, Peroxynitrite and inflammatory bowel disease, Cut 46 (2000) 436–439.
[4] P. Pacher, I.G. Obrosova, J.G. Mabley, C. Szabo, Role of nitrosative stress and peroxynitrite in the pathogenesis of diabetic complications. Emerging new therapeutical strategies, Curr. Med. Chem. 12 (3) (2005) 267–275.
[5] W.A. Pryor, G.L. Squadrito, The chemistry of peroxynitrite: a product from the reaction of nitric oxide with superoxide, Am. J. Physiol. 268 (5Pt1) (1995) L699–L722.
[6] J.I. Kourie, Interaction of reactive oxygen species with ion transport mechanisms, Am. J. Physiol. 275 (1Pt1) (1998) C1–C24.
[7] Y. Kucherenko, J. Browning, A. Tattersall, J.C. Ellory, J.S. Gibson, Effect of peroxynitrite on passive K^+ transport in human red blood cells, Cell Physiol. Biochem. 15 (6) (2005) 271–280.
[8] C. Szabo, Multiple pathways of peroxynitrite cytotoxicity, Toxicol. Lett. 140–141 (2003) 105–112.
[9] Y. Liu, D.D. Gutterman, Oxidative stress and potassium channel function, Clin. Exp. Pharmac. Physiol. 29 (4) (2002) 305–311.

[10] S. Pal, K. He, E. Aizenman, Nitrosative stress and potassium channel-mediated neuronal apoptosis: is zinc the link? Pflugers Arch. 448 (3) (2004) 296–303.
[11] X.D. Tang, H. Daggett, M. Hanner, M.L. Garcia, O.B. McManus, N. Brot, H. Weissbach, S.H. Heinemann, T. Hoshi, Oxidative regulation of large conductance calcium-activated potassium channels, J. Gen. Physiol. 117 (3) (2001) 253–274.
[12] R. Radi, J.S. Beckman, K.M. Bush, B.A. Freeman, Peroxynitrite oxidation of sulfhydryls: The cytotoxic potential of superoxide or nitric oxide, J. Biol. Chem. 266 (7) (1991) 4244–4250.
[13] M.T. Gladwin, J.R. Lancaster Jr., B.A. Freeman, A.N. Schechter, Nitric oxide's reactions with hemoglobin: a view through the SNO-storm, Nat. Med. 9 (5) (2003) 496–500.
[14] A. Dejam, C.J. Hunter, M.M. Pelletier, L.L. Hsu, R.F. Machado, S. Shiva, G.G. Power, M. Kelm, M.T. Gladwin, A.N. Schechter, Erythrocytes are the major intravascular storage sites of nitrite in human blood, Blood 106 (2) (2005) 734–739.
[15] P. Kleinbongard, R. Shulz, T. Rassaf, T. Lauer, A. Dejam, T. Jax, I. Kumara, P. Gharini, S. Kabanova, B. Ozuyaman, H.G. Schnurch, A. Godescke, A.A. Weber, M. Robenek, H. Robenek, W. Bloch, P. Rosen, M. Kelm, Red blood cells express a functional endothelial nitric oxide synthase, Blood 107 (7) (2006) 2943–2951.
[16] A. Grzelak, J. Mazur, G. Bartosz, Peroxynitrite activates K^+-Cl^- cotransport in human erythrocytes, Cell. Biol. Int. 25 (11) (2001) 1163–1165.
[17] C. Mallozzi, A.M. Di Stasi, M. Minetti, Peroxynitrite modulates tyrosine-dependent signal transduction pathway of human erythrocyte band 3, FASEB J. 11 (14) (1997) 1281–1290.
[18] P. Muriel, G. Castaneda, M. Ortega, F. Noël, Insights into the mechanism of erythrocyte Na^+/K^+-ATPase inhibition by nitric oxide and peroxynitrite anion, J. Appl. Toxicol. 23 (4) (2003) 275–278.
[19] P. Matarrese, E. Straface, D. Pietraforte, L. Gambardella, R. Vona, A. Maccaglia, M. Minetti, W. Malorni, Peroxynitrite induces senescence and apoptosis of red blood cells through the activation of aspartyl and cysteinyl proteases, FASEB J. 19 (3) (2005) 416–418.
[20] C. Mallozzi, L. De Franceschi, C. Brugnara, A.M. Di Stasi, Protein phosphatase 1 alpha is tyrosine-phosphorylated and inactivated by peroxynitrite in erythrocytes through the src family kinase fgr, Free Rad. Biol. Med. 38 (12) (2005) 1625–1636.
[21] A. Grzelak, M. Soszynski, G. Bartosz, Inactivation of antioxidant enzymes by peroxynitrite, Scand J Clin. Lab. Invest. 60 (4) (2000) 253–258.
[22] A. Denicola, J.M. Souza, R. Radi, Diffusion of peroxynitrite across erythrocyte membranes, Proc. Natl. Acad. Sci. USA 95 (17) (1998) 3566–3571.
[23] P. Di Mascio, B. Dewez, C.R.S. Garcia, Ghost protein damage by peroxynitrite and its protection by melatonin, Braz. J. Med. Biol. Res. 33 (1) (2000) 11–17.
[24] N. Romero, R. Radi, E. Linares, O. Augusto, C.D. Detweiler, R.P. Mason, A. Denicola, Reaction of human hemoglobin with peroxynitrite, J. Biol. Chem. 278 (45) (2003) 44049–44057.
[25] P.B. Dunham, J.C. Ellory, Passive potassium transport in low potassium sheep red cells: dependence upon cell volume and chloride, J. Physiol. 318 (1981) 511–530.
[26] N. Almqvist, Fractal analysis of scanning probe microscopy images, Surf. Sci. 355 (1996) 221–228.
[27] S.R. Powell, The antioxidant properties of zinc, J. Nutr. 130 (5S Suppl) (2000) 1447S–1454S.
[28] M. Valko, H. Morris, M.T. Cronin, Metal, toxicity and oxidative stress, Curr. Med. Chem. 12 (10) (2005) 1161–1208.
[29] A. Daiber, M. Bachschmid, J.S. Beckman, T. Munzel, V. Ullrich, The impact of metal catalysis on protein tyrosine nitration by peroxynitrite, Biochem. Biophys. Res. Com. 317 (3) (2004) 873–881.
[30] F. Candan, F. Gultekin, F. Candan, Effect of vitamin C and zinc on osmotic fragility and lipid peroxidation in zinc-deficient haemodialysis patients, Cell. Biochem. Funct. 20 (2) (2002) 95–98.
[31] J.A. Browning, H.M. Stains, H.C. Robinson, T. Powell, J.C. Ellory, J.S. Gibson, The effect of deoxygenation on whole-cell conductance of red blood cells from healthy individuals and patients with sickle cell disease, Blood 109 (6) (2007) 2622–2629.
[32] H.L. Brooks, J.W. Regan, A.J. Yool, Inhibition of aquaporin-1 water permeability by tetraethylammonium: involvement of the loop E pore region, Mol. Pharmacol. 57 (5) (2000) 1021–1026.
[33] K. Kuang, J.F. Haller, G. Shi, F. Kang, M. Cheung, P. Iserovich, J. Fischbarg, Mercurial sensitivity of aquaporin 1 endofacial loop B residues, Protein Sci. 10 (8) (2001) 1627–1634.
[34] F. Lapaix, S. Egee, L. Gibert, G. Decherf, S.L. Thomas, ATP-sensitive K^+ and Ca^{2+}-activated K^+ channels in lamprey (*Petromyzon marinus*) red blood cell membrane, Pflugers Arch. 445 (1) (2002) 152–160.
[35] G. Scorza, M. Minetti, One-electron oxidation pathway of thiols by peroxynitrite in biological fluids: bicarbonate and ascorbate promote the formation of albumin disulphide dimers in human blood plasma, Biochem. J. 329 (Pt2) (1998) 405–413.
[36] C.W. Haest, T.M. Fischer, G. Plasa, B. Deuticke, Stabilization of erythrocyte shape by a chemical increase in membrane shear stiffness, Blood Cells 6 (3) (1980) 539–553.
[37] E. Bossy-Wetzel, M.V. Talantova, W.D. Lee, M.N. Scholzke, A. Harrop, E. Mathews, T. Gotz, J. Han, M.H. Ellisman, G.A. Perkins, S.A. Lipton, Crosstalk between nitric oxide and zinc pathways to neuronal cell death involving mitochondrial dysfunction and p38-activated K^+ channels, Neuron 41 (3) (2004) 351–365.
[38] Y. Gutierrez-Martın, F.J. Martın-Romero, F.A. Inesta-Vaquera, C. Gutierrez-Merino, F. Henao, Modulation of sarcoplasmic reticulum Ca^{2+}-ATPase by chronic and acute exposure to peroxynitrite, Eur. J. Biochem. 271 (13) (2004) 2647–2657.
[39] G.A. Petsko, D. Ringe, Protein Structure and Function, New Science Press Ltd., London, 2004, pp. 86–127.
[40] J.S. Gibson, J.C. Ellory, K^+-Cl^- cotransport in vertebrate red cells, in: I. Bernhardt, J.C. Ellory (Eds.), Red Cell Membrane Transport in Health and Disease, Springer, Berlin, 2003, pp. 197–220.
[41] F. Lesage, M. Lazdunski, Molecular and functional properties of two-pore-domain potassium channels, Am. J. Physiol. Renal. Physiol. 279 (5) (2000) F793–F801.